A DESIGN MODEL FOR WATERBOUND MACADAM BASED ON HEAVY VEHICLE SIMULATOR AND LABORATORY TEST RESULTS

H L Theyse, E Sadzik and J P Notnagel

Transportek CSIR, P O Box 395, Pretoria, 0001
GAUTRANS, Private Bag X3, Lynn East 0039
SANRAL, Private Bag X5, Alkantrant 0005

INTRODUCTION

Transportek recently completed a draft guideline document on the selection, design and construction of waterbound macadam pavements which was co-funded by the Gauteng Department of Transport and Public Works (GAUTRANS) and the South African National Road Agency Limited (SANRAL). One of the objectives of the project was to develop a rational design method for waterbound macadam from existing Heavy Vehicle Simulator (HVS) data and laboratory test results and to incorporate the new design method into the South African Mechanistic-empirical Design Method (SAMDM). Previous publications on the SAMDM did not include any information on the mechanistic-empirical design of waterbound macadam pavement layers. The information presented in this document is additional to the SAMDM (1) and should be used in conjunction with the SAMDM. The following items are covered:

- recommendations on the load sensitivity of waterbound macadam base layers,
- recommendations on the stiffness input parameters required by the SAMDM for waterbound macadam material and
- design transfer functions for the mechanistic-empirical design of pavements with waterbound macadam base layers.

The data on which the above recommendations are based were obtained from Heavy Vehicle Simulator (HVS) test data and triaxial laboratory test data. The design transfer functions were developed from laboratory test results for two practical cases which may be encountered on waterbound macadam construction projects:

- The first case is for a WM2 (2) waterbound macadam base layer constructed on a granular subbase or relatively thin cement-treated subbase. Because of the relatively weak compaction platform provided by the subbase, the base layer is at 84 % of apparent density. Because of the lower density, the saturation level of the base layer is about 30 % for normal moisture conditions.

- The second case is for a WM1 (2) waterbound macadam base layer which is constructed on a sufficient compaction anvil consisting of at least 125 mm cement-treated material and the base density is 88 % of apparent density. Because of the low voids content, the saturation level of the base layer is about 45 % for normal moisture conditions.

The laboratory design models showed good correlation with field test results from the HVS but seem to underestimate the load sensitivity of waterbound macadam. The results from HVS tests were therefore used to investigate the load sensitivity of waterbound macadam base layers. HVS test results also contributed to the general information available on waterbound macadam and results from the following HVS tests were used in this investigation:

- Gauteng — HVS tests 400a4 and 402a4 done near Cullinan (3)
- Northern Province — HVS tests 404a4 and 405a4 done near Louis Trichardt (4)
- KwaZulu-Natal — HVS test 329a3 done near Umkomaas (5)
  HVS tests 128a3 and 178a3 at Marianhill, Pinetown (6)
  HVS tests 362a3 and 366a3 at Seaslopes, Margate (7)

A brief description of the results from the HVS tests at these locations is given with specific emphasis on information that is pertinent to the objectives of the guideline document.

HVS TEST RESULTS ON WATERBOUND MACADAM

HVS tests 123a3, 124a3, 128a3 and 178a3 at Marianhill, Pinetown

These HVS test sections were situated on Main Route 85 (MR85) near Marianhill, Pinetown. A crusher sand was used as the filler for the waterbound macadam base layer of these sections. Initially, the only difference between sections 123a3, 124a3 and 128a3 and section 178a3 was the thickness of the pavement layers. After the disappointing HVS test performance (6) of sections 123a2, 124a3 and 128a3 (which was constructed without slushing the waterbound macadam base layer), it was decided to recompact the base layer of section 178a3 by using a slushing process. More detail on the effect of the slushing process will follow later.

The structural detail of the two test sections are as follows:

Sections 123a3, 124a3 and 128a3	Section 178a3
50 mm continuously graded asphalt	65 mm continuously graded asphalt
150 mm waterbound macadam	235 mm waterbound macadam
150 mm C1 cement-treated crushed stone	125 mm C1 cement-treated crushed stone
150 mm C3 cement-treated sandstone	125 mm C3 cement-treated sandstone
600 mm dumprock and sandstone	600 mm dumprock and sandstone

The test programme for section 123a3 consisted of 890 000 load repetitions at 70 kN with a tyre inflation pressure of 600 kPa of which the last 60 000 repetitions were applied with water entering the base layer through 38 mm diameter perforated pipes which were inserted into the layer. 600 000, 100 kN load repetitions at 600 kPa inflation pressure was applied to section 124a3 with water being applied from 480 000 load repetitions onwards. Water was applied to the base layer of section 128a3 for the full 600 000 load repetition duration of the test. The trafficking load was increased from 40 kN at 600 kPa inflation pressure to 60 kN at the same tyre pressure from 220 000 repetitions onwards. The trafficking load for test 178a3 on the thicker waterbound macadam base layer was 100 kN at 600 kPa inflation pressure for 973 000 load repetitions with water being applied from 600 000 repetitions onwards.

The surface rut for test section 123a3, 124a4 and 128a3 increased rapidly so that all these sections reached a rut of 20 mm within 400 000 load repetitions of their respective trafficking loads. In all three cases the rapid deformation of these sections seems to be related to either rain water entering the base layer or the water applied during the test. This indicates that although waterbound macadam may act as a drainage layer, the performance of the layer will be affected by the presence of excess moisture. The density of the waterbound

macadam layer was also not sufficient, in addition to the influence that the moisture condition had on the performance of these test sections. The density outside the HVS test section for test 128a3 was 84 per cent of Apparent Density (AD) and this density is believed to be representative of the density before testing. The density increased to 89,5 per cent of AD after the HVS test was completed. The poor performance of sections 123a3, 124a3 and 128a3 may therefore be ascribed to the combined effect of low density and high moisture content.

Based on the poor performance of the HVS sections tested on this site, a decision was taken to recompact section 178a3 before HVS testing (8). The additional compaction basically consisted of rolling and vibration of the layer followed by the slushing of the layer. The density of section 178a3 before recompaction was 85 per cent of AD and increased to 86 per cent with additional rolling and then increased further to 88,6 per cent after slushing. The additional benefit of slushing is thus clearly illustrated by these data. The density of section 178a3 increased slightly more to about 90 per cent of AD under HVS trafficking.

The increased density of section 178a3 had a marked effect on the water absorbed by the layer through the perforated pipes installed in the layer (8). The average water absorption was 15 litre/hour/hole for the low density sections 123a3,124a3 and 128a3 and 0,15 litre/hour/hole for the high density section 178a3.

The higher density and hence lower water absorption of section 178a3 resulted in significantly better performance with the section only reaching 20 mm rut at about 1 million 100 kN load repetitions (6). The waterbound macadam layer was, however, again the main contributor to the permanent deformation of all four of the test sections.

Horak calculated the bearing capacity of sections 123a3 and 124a3 as ranging from about 3 to 12 million standard axles with that of section 128a3 being even lower at between 0,8 and 3 million because of the higher moisture level in section 128a3. The bearing capacity of section 178a3 was calculated as being between 10 and 20 million standard axles.

HVS test 329a3 near Umkomaas

Based on the encouraging results fromHVS test section 178a3 near Marianhill, the then Natal Provincial Administration decided to build a 13 km length of dual carriageway on the N2 near Umgababa during 1985, using a base course of waterbound macadam with a natural sand filler. HVS test section 329a3 was located on this section of road. A second section with a crushed stone base layer was also constructed close to the waterbound macadam section and tested with the HVS to enable a comparison of the performance of the two base layer types.

The pavement structure consisted of the following:

40 mm semi-gap graded wearing course combined with a 25 mm continuously graded levelling course
150 mm waterbound macadam base layer
125 mm cement-treated crushed stone subbase
125 mm lime stabilised gravel subbase
150 mm G7 subgrade
150 mm G9 subgrade
G10 subgrade

The HVS test was started off with a 100 kN trafficking load for 794 000 repetitions after which holes were drilled through the surfacing and into the base layer for water to enter the base layer and the trafficking load was reduced to 40 kN. The trafficking load was again increased to 100 kN from just less than 1,3 million repetitions to the end of the test at 1,721 million repetitions.

Again, as was the case with the test sections at Marianhill, the waterbound macadam base layer contributed the largest portion (between 45 and 60 %) of the total permanent deformation of the pavement structure. Wright and Hess (5) calculated the bearing capacity of the HVS test section at between 14 and 16 million standard axle loads. The rate of deformation of the G1 crushed stone test section was lower than that of the waterbound macadam with the G1 section having half the rut (11 mm against 22 mm) of the waterbound macadam section after completion of a similar test programme.

HVS tests 362a3 and 366a3 at Seaslopes, Margate

The only difference between sections 362a3 and 366a3 is the 40 mm asphalt wearing course that was placed on section 366a3 whereas only a 10 mm slurry wearing course was placed on section 362a3. Both sections have penetration macadam base layers which is in essence a waterbound macadam base with about the top 25 mm of the layer being penetrated with slurry. The pavement structures of these two test sections consist of the following:

10 mm slurry wearing course for section 362a3 and 40 mm asphalt wearing course for section 366a3
25 mm penetration slurry
125 mm waterbound macadam base layer
150 mm C2 cement-treated subbase
no detail is available on the support layers

The bearing capacity of section 362a3 was calculated from the HVS test by Roux and Otte (7) as 3,7 million standard axles and that of section 366a3 as 7,5 million standard axles. Again the main contribution to the total permanent deformation of the pavement section came from the waterbound macadam base layer. The relatively poor performance of these two sections in comparison with the other waterbound macadam sections cited in this report was not explained by Roux and Otte. McCall et al (9) did, however, mention problems with construction water that was trapped in the waterbound macadam base layer of the section of road on which the HVS test sections were situated because of blocked side drains. A high moisture content may therefore have been the cause of the relatively poor performance of these test sections.

HVS tests 400a4 and 402a4 near Cullinan

Sections 400a4 and 402a4 had waterbound macadam base layers of 100 and 150 mm thickness respectively. The base layers were constructed using a 53 mm nominal size coarse aggregate and a natural sand filler. The detail of the pavement structures of these two test sections is given below:

Section 400a4	Section 402a4
30 mm continuously graded asphalt	30 mm continuously graded asphalt
100 mm waterbound macadam	150 mm waterbound macadam
150 mm C4/G4 sandstone material	150 mm C4/G4 sandstone material
300 mm G4 sandstone	300 mm G10 ferricrete

The quality of the ferricrete selected subgrade of section 402a4 was of a much lower quality than the sandstone selected subgrade of section 400a4. The density of the waterbound macadam base layers of these two sections were in places as low as 78 % of AD with maximum values of 81 % of AD. (3).

Both these sections were subjected to the same test programme with 200 000 load repetitions applied at 40 kN and a tyre inflation pressure of 520 kPa. Thereafter the load was increased to 70 kN at 670 kPa inflation pressure for a further 200 000 repetitions. Water was added to one half of the section for a further 100 000 load repetitions at 70 kN.

The difference between these two test and the other HVS test case studies cited in this report is that the supporting structures of these two test sections were of a much lower standard than that of the other test sections. Whereas most of the rutting of the other test sections originated from the waterbound macadam base layers, the layers below the waterbound macadam base layers of sections 400a4 and 402a4 also contributed significantly to the total permanent deformation especially the weak ferricrete layer on section 402a4. It must, however, be kept in mind that the pavement structures of test sections 400a4 and 402a4 are intended for provincial roads and not national routes. A comparison of the bearing capacities of the full pavement structures of sections 400a4 and 402a4 with that of the full pavement structures on the other HVS test sections would therefore underestimate the bearing capacity potential of the waterbound macadam. The estimated bearing capacity of the base layers alone is therefore reported. The bearing capacity of the base layer of section 400a4 is estimated at 13 million standard axles and that of section 402a4 at 11 million standard axles.

HVS tests 404a4 and 405a4 near Louis Trichardt

These two test sections were located on a section of the N1-28 with a waterbound macadam base layer constructed by labour-intensive methods. A 73 mm nominal size coarse aggregate was used with a crusher sand filler. The pavement structure of the two sections was the same and the detail is as follows:

50 mm asphalt
125 mm waterbound macadam
300 mm C3 cement-treated weathered granite
300 mm G7 weathered granite selected subgrade

The waterbound macadam base layers of these sections were well compacted using heavy rollers and a slushing process. The density of the waterbound macadam base layer was 88 % of AD in the vicinity of the HVS test sections.

Section 404a4 was tested for 500 000 load repetitions with a dual wheel-load of 70 kN at an inflation pressure of 690 kPa. Section 405a4 was tested with a 40 kN trafficking load at 520 kPa inflation pressure for 380 000 load repetitions after which the load was increased to 100 kN at 800 kPa inflation pressure until 900 000 load repetitions was reached. Water was then added to the one half of the section for another 100 000 load repetitions.

Both the test sections performed exceptionally well under HVS testing. Although most of the permanent deformation occurred in the waterbound macadam base layer of sections 404a4 and 405a4 there was very little permanent deformation in total. The pavement bearing capacity of these two sections were estimated at about 37 million standard axle loads.

Although the general information presented above on the performance of waterbound macadam from HVS testing does not allow detailed analysis, the influence of the density and moisture content of the waterbound macadam on the performance of this material is mutual to all these tests. This is typical of the performance of unbound materials and although waterbound macadam may in some cases be used as a drainage layer, it is certainly not immune to the detrimental effects of excess moisture.

RECOMMENDATIONS ON THE STRUCTURAL DESIGN OF PAVEMENTS WITH WATERBOUND MACADAM BASE LAYERS

Load Sensitivity

Figure 1 shows the bearing capacity estimates (number of load repetitions to 20 mm rut) at different wheel loads for the base layers of a number of HVS test sections. The load sensitivity of waterbound macadam may be calculated from the data in Figure 1.

The base bearing capacity is determined by the amount of bedding-in deformation that occurs during initial trafficking and the eventual linear rate of increase in deformation of the base layer. These two parameters are shown in Figures 2(a) and (b) plotted against the applied wheel load for the HVS test sections for which permanent MDD displacement data were available. Both the bedding-in deformation and the linear deformation or plastic strain rate are expressed as a percentage of the initial base layer thickness.

The load equivalency factors and load equivalency exponents for the load equivalency law given by Equation 1 was calculated from the average of the base bearing capacity values shown in Figure 1 for the respective dual wheel load conditions. The results are summarized in Table 1.

$$LEF = \left(\frac{P}{80}\right)^{n} \qquad \text{Eq. 1}$$

Where LEF = Load Equivalency Factor
P = the applied axle load (kN) for which the LEF is calculated
n = the damage law exponent

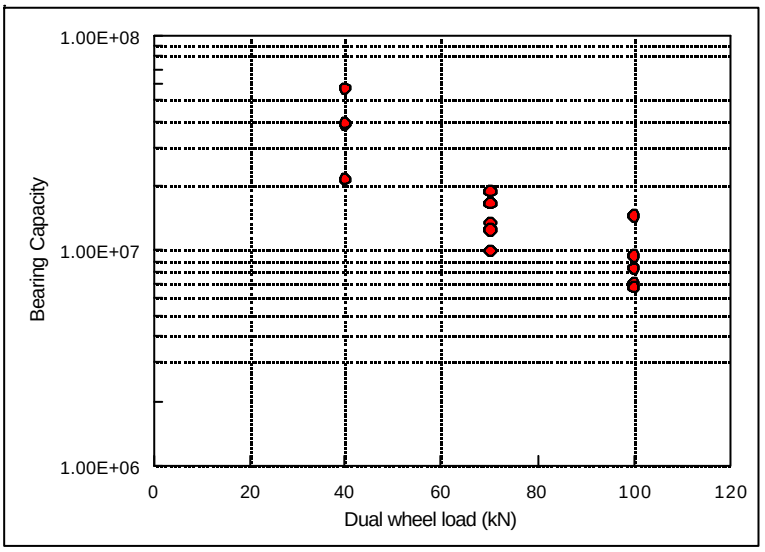

Figure 1: The load sensitivity of waterbound macadam base layers as determined from several HVS test sections

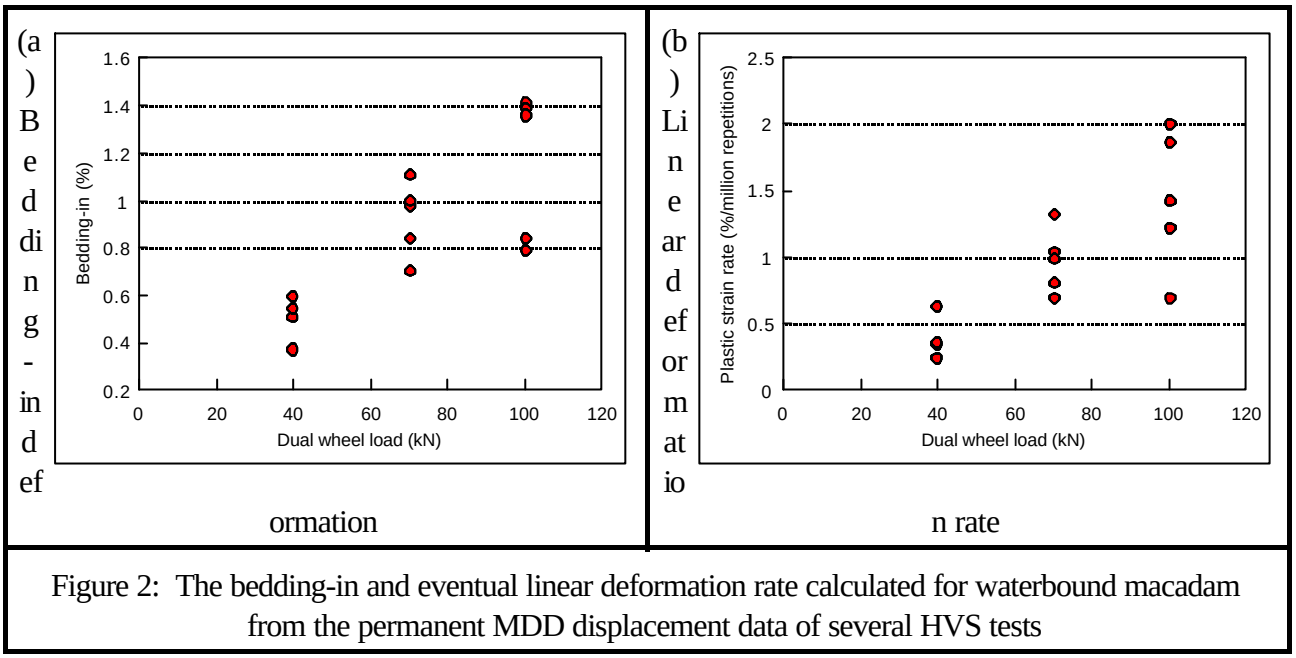

Figure 2: The bedding-in and eventual linear deformation rate calculated for waterbound macadam from the permanent MDD displacement data of several HVS tests

Table 1: Load equivalency factors and exponents for waterbound macadam base layers			
Axle load (kN)	Average Base Bearing Capacity	Load Equivalency Factor	Load Equivalency Exponent
40	39,1 million		
70	14,3 million	2,7	1,8
100	9,2 million	4,3	1,6

The results from Table 1 agrees well with similar results calculated by Horak, (6). The low values of "n" calculated for the waterbound macadam base layers are indicative of the ability of waterbound macadam to withstand high axle loads. It is, however, not only the waterbound macadam base layer that will determine the load equivalency of the total pavement structure. The calculation of the parameters shown in Table 1 was repeated using the pavement bearing capacity data of the HVS sections and a damage exponent between 1,8 and 2,0 was obtained.

The pavement structures of the HVS test sections used in this analysis are typical of the designs that will be used for waterbound macadam pavements and the low damage exponent of 2,0 therefore seems to be a realistic value for pavement structures with waterbound macadam base layers. It is therefore suggested that a value of 2,0 should be used for the damage exponent when converting actual traffic to equivalent design traffic.

Stiffness Input Parameters

Table 2 shows a summary of back-calculated effective stiffness values for waterbound macadam material from a number of HVS test sections for a 40 kN dual-wheel test load. The initial values were recorded at the beginning of the test but the effective stiffness soon reduced to values similar to the average values listed in Table 2. The effective stiffness results calculated at different positions on the HVS test sections are given for the initial and average values to indicate the spatial variability that may be expected in the effective stiffness of waterbound macadam. These values are in general higher than the values that would be expected for crushed

stone material. Hefer (10) found similar values of stiffness for waterbound macadam material using Falling Weight Deflectometer data. One of the interesting aspects of the resilient behaviour of waterbound macadam material is that for thinner layer thicknesses, the effective stiffness of the layer increases. This is because of the relatively fewer load transfer points in a thin layer with large aggregate particles in the layer. This boundary condition phenomena is not readily repeated in the laboratory unless squat samples are used.

Table 2: 40 kN test load back-calculated effective stiffness moduli for a number of HVS tests

HVS section	Effective stiffness modulus (MPa)			Comments
	Initial	Average	Wet	
329a3	873, 1144	628, 622	-	150 mm WM, reasonable support
366a3	1318, 1634	1162, 1250	-	125 mm WM, extremely good support
400a4	1517, 2031	1295, 1714	520	100 mm WM, reasonable support
402a4	481, 1104	441, 472	335	150 mm WM, poor support
404a4	465, 835	371, 629	-	125 mm WM, good support
405a4	802, 1117	480, 964	267	125 mm WM, good support

Theyse (11) did extensive static and dynamic triaxial testing of waterbound macadam material. Dynamic triaxial secant stiffness modulus data from this work were used to developed the effective stiffness (E_{eff}) model for waterbound macadam given in Equation 2. This model incorporates the effect of relative density (RD), saturation (S), confining stress ($ó_3$) and shear stress condition (SR) on the effective stiffness response of waterbound macadam and yields stiffness results comparable to those back-calculated from depth deflection data. The relative density and degree of saturation is expressed as a percentage of the apparent density and inter-particle voids respectively (88 % and 30 % for instance). The quantification of the shear stress condition by the stress ratio (SR) is explained in a subsequent section.

$$E_{eff} = -3932{,}71 + 54{,}96\,RD - 1{,}54\,S + 5{,}87\,s_3 - 3{,}07\,SR \qquad \text{Eq. 2}$$

The correlation coefficient, R^2 was 0,651. The parameters included in the model therefore explain 65,1 per cent of the variation in the effective stiffness response. The effect of compaction on the stiffness of waterbound macadam is evident from Equation 2 with the coefficient for the relative density being the highest.

Table 3 provides suggested stiffness input values for the mechanistic-empirical design of waterbound macadam material based on the model given above with allowance made for increased stiffness for thin (100 mm thick) layers.

Table 3: Suggested stiffness moduli for the mechanistic-empirical design of waterbound macadam base layers					
Material code	Layer thickness (mm)	Dry condition (30 - 45 % saturation)		Moist condition (60 % saturation)	
		Well supported by an intact cemented-treated subbase creating confinement of the waterbound macadam layer	Relatively weak support provided by a granular or equivalent granular subbase layer	Well supported by an intact cemented-treated subbase creating confinement of the waterbound macadam layer	Relatively weak support provided by a granular or equivalent granular subbase layer
WM1	100	1200	800	1100	640
	> 100	1080	620	1010	550
WM2	100	1000	600	900	440
	> 100	880	420	790	330

Design Transfer Functions

The transfer functions of a mechanistic-empirical design method contains the performance data for a particular road-building material and these transfer functions need to be calibrated using measured performance data. The performance in terms of permanent deformation of waterbound macadam using crusher sand and natural sand fine aggregate was tested using the dynamic triaxial test (11). Bearing capacity estimates obtained from this study agreed well with HVS bearing capacity estimates for a standard design axle load of 80 kN. It was therefore decided to use the laboratory derived design model for the mechanistic-empirical design of waterbound macadam as it allow much wider variation in density and saturation levels than HVS test data do.

There are, however, two components to the design model. Firstly, the static shear strength parameters of the material need to be known and secondly the performance of the material needs to be known for a range of stress conditions. As waterbound macadam is basically an unbound material, permanent deformation is the dominant mode of distress of this material as was highlighted by the HVS test results from the previous section.

Equation 3 gives the model that was obtained for the friction angle (ö) of waterbound macadam material as a function of the relative density (RD) and saturation (S) of the material. The relative density and saturation is expressed as a percentage of the apparent density and inter-particle voids respectively (88 % and 30 % for instance).

$$f = -26{,}38 + 1{,}021\,RD - 0{,}171\,S \qquad \text{Eq. 3}$$

The correlation coefficient (R^2) for the model was 0,981. Again, the relative density has the biggest influence on the value of the friction angle. The cohesion (C) of the waterbound macadam material was found not to be a function of the density or saturation and an average value of 74 kPa was obtained for the cohesion. Figure 3 illustrates the relationship between the friction angle, density and saturation of waterbound macadam material.

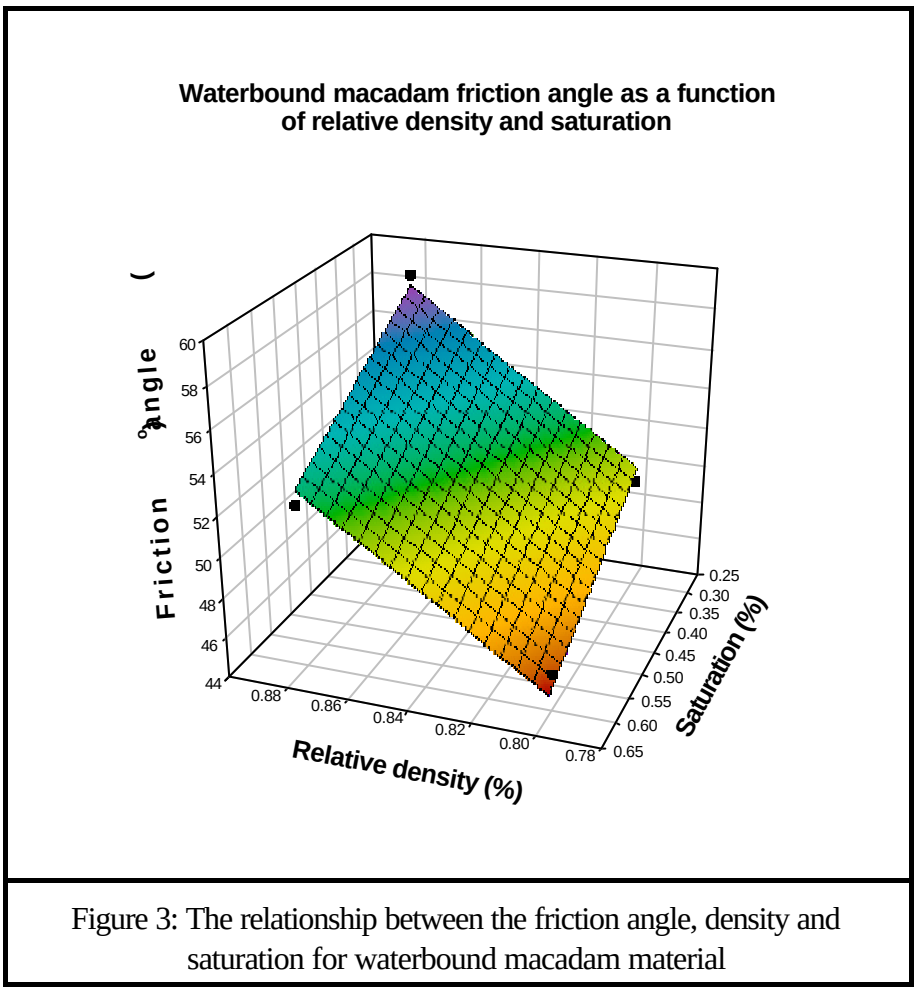

Figure 3: The relationship between the friction angle, density and saturation for waterbound macadam material

The friction angle values obtained for the waterbound macadam material is not any higher than the friction angle values expected for crushed stone material. The values obtained by Theyse (11) were verified with additional testing at Spoornet's track testing facility. The previous assumption that the friction angle of waterbound macadam should exceed that of crushed stone and that the permanent deformation performance of waterbound macadam should therefore exceed that of crushed stone is therefore not valid. The work done by Theyse (11) has, however, also indicated that static shear strength parameters are not unique indicators of performance under dynamic loading. Materials with excellent static shear strength have performed poorly under HVS and dynamic triaxial testing. The maximization of the static shear strength parameters for a particular material type through achieving the maximum practical density and the lowest practical saturation will, however, ensure the best permanent deformation performance for that material.

Equation 4 provides the formula for calculating the bearing capacity in terms of the number of axle load repetitions (N) that can be sustained before a certain level of plastic strain (PS) is induced in waterbound macadam material from the dynamic triaxial test results by Theyse (11). The definition of RD, S and SR is as given previously. The model is based on the combined dynamic triaxial test data for waterbound macadam material with crusher sand and natural sand filler. The stress ratio (SR) is analogous to the previously used safety factor for unbound materials and the definition of the stress ratio is given in Equation 5.

$$log\ N = 1{,}891 + 0{,}075\ RD - 0{,}009\ S + 0{,}028\ PS - 1{,}643\ SR \qquad \text{Eq. 4}$$

$$SR = \frac{\sigma_1^a - \sigma_3}{\sigma_1^m - \sigma_3} = \frac{\sigma_1^a - \sigma_3}{\sigma_3\left(\tan^2\left(45 + \frac{\phi}{2}\right) - 1\right) + 2C\tan\left(45 + \frac{\phi}{2}\right)} \qquad \text{Eq. 5}$$

Where σ = principal stress (kPa)
τ = shear stress (kPa)
ϕ = internal angle of friction (°)
C = cohesion (kPa)
σ_1^m = maximum allowable major principal stress given ϕ, C and σ_3 (kPa)
σ_1^w or σ_1^a = working or applied major principal stress (kPa)
σ_3 = minor principal stress or confining pressure (kPa)

The correlation coefficient for the model given in Equation 5 is 0,822 and a graph of the predicted bearing capacity values plotted against the observed values is shown in Figure 4.

Equation 4 provides a general design model for waterbound macadam. If the conditions for the two design scenarios from the Introduction are substituted in Equation 4 and the plastic strain is expressed in terms of a 20 mm rut which is the terminal condition for permanent deformation, Equations 6 and 7 are obtained. These equations serve as the basis for the mechanistic-empirical design of waterbound macadam base layers with thickness between 100 and 150 mm for the two design scenarios. Draft TRH4 (12) stipulates the approximate design reliability for different road categories and the South African Mechanistic-empirical Design Method incorporate design reliability by using transfer functions at certain offsets from the basic model, based on the distribution of the data around the basic model. The offsets obtained from the analysis of the residuals of the model given in Equation 4, are given in Table 4 and should be used for the design of pavements for different road categories.

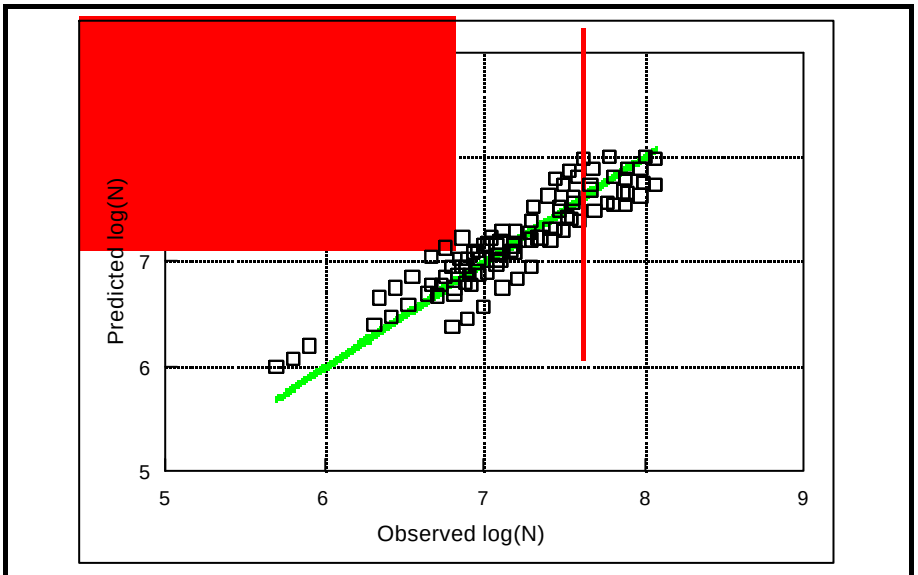

Figure 4: Predicted bearing capacity plotted against observed bearing capacity for waterbound macadam material with either a crusher sand or natural sand filler

Conditions for the 1st design case:
Relative density: 84 %
Saturation: 30 %
Design model:

$$logN = 7{,}905 + 0{,}028\left(\frac{20}{t} \times 100\right) - 1{,}643SR \qquad \text{Eq. 6}$$

Conditions for the 2nd design case:
Relative density: 88 %
Saturation: 45 %
Design model:

$$logN = 8{,}086 + 0{,}028\left(\frac{20}{t} \times 100\right) - 1{,}643SR \qquad \text{Eq. 7}$$

Where "t" is the thickness of the base layer in mm.

Table 4: Offsets from the basic design models to be used for the design of pavements for different road categories

Road category	Approximate design reliability	Offset (to be subtracted from the constants in Equations 6 and 7)
A	95 %	-0,29
B	90 %	-0,23
C	80 %	-0,16
D	50 %	-0,03

Figure 5 shows contour plots of the general design model from Equation 4 for relative density values of 84 and 88 per cent and a saturation level of 45 per cent. The effect of an increase in density on the bearing capacity of the waterbound macadam layer is illustrated by comparing the bearing capacity results at a stress ratio value of 50 per cent for the two cases.

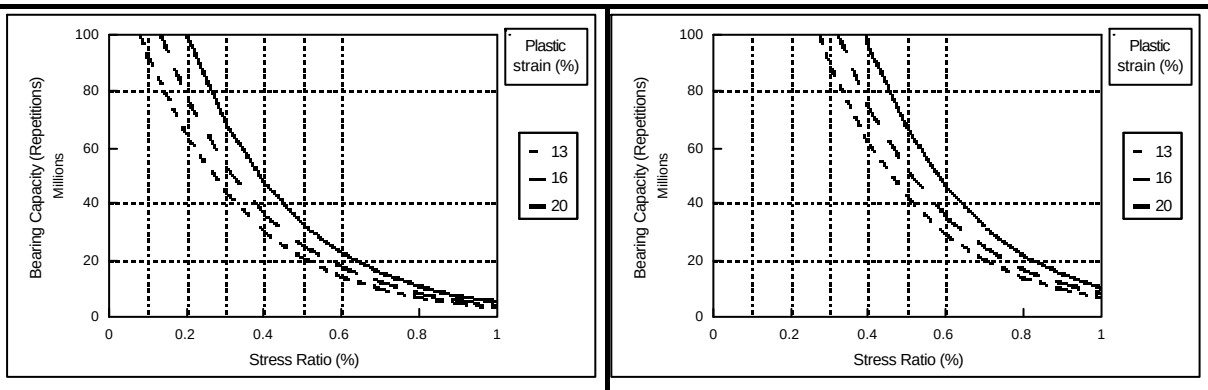

(a) 84 % relative density, 45 % saturation

(b) 88 % relative density, 45 % saturation

Figure 5: The effect of density on the bearing capacity of waterbound macadam

The bearing capacity for 13 per cent plastic strain which is equivalent to 20 mm permanent deformation of a 150 mm layer doubled from about 20 million standard axle loads for the 84 % relative density case to 40 million standard axle loads for the 88 % relative density case. This comparison is done at the same stress ratio for both cases. The shear strength of the material will, however, increase with an increase in density, resulting in a lower stress ratio for the high density case which will lead to an even larger increase in bearing capacity.

CONCLUSIONS AND RECOMMENDATIONS

The design model for waterbound macadam material presented in this paper is based on a combination of Heavy Vehicle Simulator data and laboratory test data. The laboratory data supplemented the HVS test data by widening the range of the variables over which the data was collected. The impact of this on the design model is that the effect of density and saturation could be included in the design model for both the effective stiffness and permanent deformation response of the waterbound macadam material.

The effective stiffness results for the waterbound macadam from both HVS back-calculation and laboratory test results indicate that the stiffness of waterbound macadam is higher than typical values expected for a crushed stone material.

The friction angle of waterbound macadam is not higher than the friction angle of crushed stone as was expected previously. The permanent deformation response of unbound aggregate is, however, not uniquely determined by the static shear strength parameters of the material although the permanent deformation of the material will be minimized by maximizing the static shear strength parameters. By achieving maximum practical density and the lowest degree of saturation possible under field conditions, the permanent deformation of waterbound macadam will be the least as it will be for other unbound aggregates.

The rational design model for waterbound macadam presented in this paper was incorporated in the SAMDM for the design of different road categories at different design reliability levels. A design catalogue based on this design model was incorporated into a guideline document on the selection, design and construction of waterbound macadam base layers.

REFERENCES

1. Theyse H L and Muthen M. *Pavement Analysis and Design (PADS) Software based on the South African Mechanistic-empirical Design Method*. Paper accepted for publication at the Annual Transportation Convention, Pretoria. 2000.

2. Committee of State Road Authorities (CSRA), 1985. *TRH14 Guidelines for road construction materials*. Department of Transport. Pretoria. 1985.

3. Theyse H L. *The Evaluation of Pavements with Labour-intensively Constructed Base Layers, a Case Study on Road 2388*. Proceedings of the 7th Conference on Asphalt Pavements for Southern Africa, Victoria Falls, Zimbabwe. 1999.

4. Theyse H L. *First level report for HVS testing on the N1-28 near Louis Trichardt. Transportek*, Transportek, CSIR, Pretoria. 1999. (Report no. CR-99/065).

5. Wright B and Hess R. *Evaluation of a freeway pavement incorporating a waterbound macadam base*. Division of Roads and Transport Technology, Pretoria. 1988.

6. Horak E. *Watergebindemacadamplaveisels*. M Eng Thesis, University of Pretoria. 1983.

7. Roux P L and Otte J R. *Coarse aggregate bases*. Transportek, CSIR, Pretoria. 1983. (RDAC report RR 88/027)

8. Horak E. *The recompaction of the 250 mm thick experimental waterbound macadam section at Marianhill, Pinetown*. National Institute for Transport and Road Research, Pretoria. 1982. (Technical Note: TP/72/82)

9. McCall J, Roux P and Currie R. *Waterbound macadam in single carriageway highway construction in Natal*. Proceedings of the Annual Transportation Convention, Pretoria. 1990.

10. Hefer A W. *Towards design guidelines for macadam pavements*. M Eng Thesis, University of Pretoria. 1997.

11. Theyse H L. *Laboratory design models for materials suited to labour-intensive construction, Volume I: Report*. Transportek, CSIR, Pretoria. 1999. (Confidential contract report CR-99/038)

12. Committee of Land Transport Officials (COLTO). *Draft TRH4 1996: Structural design of flexible pavements for inter-urban and rural roads*. Department of Transport, Pretoria. 1996.